Study of the flagellar movement in biology with applications in MEMS and micro robotics

Author:
Constantin Alexandru
Coordinators:
Prof. Simona Vasilescu
Dr.Ing. Mircea Ignat
High School:
"Tudor Vianu" National High School of Computer Science
Bucharest

Contents

I. Introduction

The theme is essentially a research topic specific to the field of bionics. That is, an approach based on biological research with specific technical or engineering results.
Thus, the research approach algorithm will include the detailed study of the microbiological structure of flagellates with weight on the microsystem of movement represented by flagellum. Continuing with simple static, cinematic or dynamic models, a study is made on various types of existing electromechanical actuators based on conventional or unconventional drivers;
- Electromagnetic microactuators;
- Micro-motors D.C. or A.C.
- Piezoelectric actuation
- Electrostrictive actuation,
- Electrodynamic actuation,
- Magnetostrictive actuation,

The study of these types of actuators will be made comparative in the idea that priorities are set in the realization of primary experimental models which after laboratory experiments will have special actuation performances; speeds, accelerations, etc.
It then returns to the optimization of the initial (or primary) microelectromechanical models, eventually reaching patentation of calculation and design. On this basis, several optimized experimental models will be built.
For achieving experiments, experimental protocols and small specific stands will be established, such as; hydrodynamic micro-tunes, micro dynamometer measuring systems to determine fluid forwarding forces, micro frequency, forward, flotation, etc.
The last chapter is dedicated to dissemination, research in the sense of finalizing published or communicated scientific works, or the completion of some patent proposals, adding new research topics, starting from the present research, according to the scientific spirit (see Bachelard) to continue a research.

II. Biological Structure

II.1 Systematic classification

Protista is the most controversial group of living organisms because it has a complex and heterogeneous structure; includes eukaryotic, unicellular, colonial, heterotrophic, identical or similar to the ancestors of current plants, fungi and animals. In the Protista kingdom there are protozoa, algae, myxomycetes and oomycetes. Protozoa (from: protos = first and zoon = animal) are micro-organisms, exclusively unicellular, that lead a free life (eg Ciliophora), usually in aquatic environments. Each protozoan functions as an independent entity capable of accomplishing all the activities necessary for life. All cells are structurally and physiologically similar, as a result there is a certain equivalence between the unicellular body of the protozoa and the multicellular body of the animals. If the body of an animal compares with that of a protozoan, it is obvious that structurally, protozoan has a much simpler organization. Instead, the cell that forms the body of a protozoan has a much more complex organization, because this single cell fulfills all the processes of life, while the cells in the animal organisms are strictly specialized in fulfilling only a certain function. The most important protozoa, both theoretically and socio-economically, are flagellates, including the Euglenoids common organisms in freshwater aquatic basins, rich in organic matter. The typical representative is Euglena (Fig.1).

II.2 Cell Structure (Euglena)

The protozoan cell has a typical eukaryotic organization, consisting of membrane, cytoplasm and nucleus. Euglena virdis is a protist with an elongated, navicular body, pointed at one end. One end is extended with a long and thin flagllum [I.13]. Her body is covered by a pellicle (thick and strong membrane), for this reason the shape of the body is constant and it does not deform.

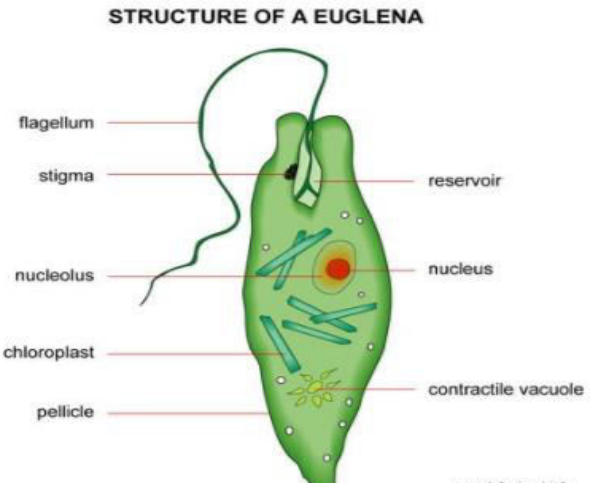

Fig.1 Structure of Green Euglena[III.7]

Inside the body is distinguished the large, spherical nucleus, located in the anterior region surrounded by chromatin granules. At the posterior end there is a red spot called stigma, it is photosensitive and acts as an "eye" or orientation organ.

Next to the stigma, at the anterior end is a funnel-shaped cytostome or cell mouth slightly to one side of the centre. Cytostome leads into a short tubular cytopharynx or gullet which, in turn, joins a large spherical vesicle, the reservoir or flagellar sac. The cytostome and cytopharynx are not used for ingestion of food but as a canal for escape of fluid from the reservoir**.** The root of the flagellum is bifurcated and each branch ends with a small, round basal granule, called belpharoplast[III.2].

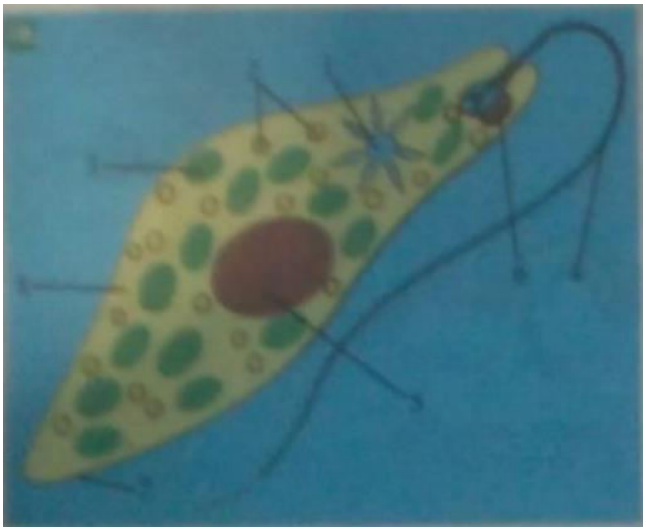

Fig.2 Green euglena; 1- pulsatile vacuole; 2- digestive vacuoles; Chloroplast; 4- flagellum; 5-nucleus; 6- stigma; 7- membrane; 8- cytoplasm[I.1].

II.3 Functions of the body

a. Nutrition function [I.12]

Due to the sensitivity to light, it feeds holophytically synthesizing O2 with the chloroplasts. When external light conditions do not allow euglena to feed on autotroph, it eats organic substances that it takes from the aquatic environment, making an inherent heterotrophic feeding. The movement of the flagellum produces currents in water that draw the food to its base, from which it is processed. Being a descendant of herbs, Euglena breathes taking $O_2$and yields CO_2. This process takes place across the surface of its membrane. Excretion is by membrane by means of excretion vacuole.

b. Reproduction function

- Protozoa are reproduced asexually by longitudinal or transversal binary division of cells (scissiparity or split), and sometimes also sexed by fusion of two cells that have gametes function. Every cell is capable of reproducing. Under unfavorable conditions the phenomenon of cell closure (dehydration and secretion of a resistant coating) occurs. Cyst is the form of resistance under which the protozoan passes over the unfavorable periods.

Fig.3 Longitudinal binary division at euglena[I.1]

c. Relationship function

It is manifested by two characteristics - the sensitivity that is achieved through the membrane and the stigma and the locomotion that is realized with the help of the flagellum.

III. Movement explanation and static micromechanical structures

Euglena moves actively with the flagellum at speeds of up to 20-60 μm / s. The ciliary motion efficiency can be expressed by the following example: Paramecium caudatum ciliary infuser advances in one second in water by pumping the cilia at a rate of 4-6 times the length of its body, while an Olympic swimmer does only once per second [I.1]. Eukaryotic cilia and flagellums are the filiform cytoplasmic structures, emerging at the cell surface, representing specific organisms of movement in liquid media. In connection with its function, the flagellum has a special structure. It consists of an axial filament made up of several longitudinal fibers and a pretoplasmic sheath covering provided with a spiral filament surrounding the axial filament. On the pellicle, there are extremely fine petioles, called mastigones, which are regularly displacled on a single row along the flagellum. The flagellum performs core-to-peak wave propagation movements in one plane. There are two fundamental effects of flagellar and ciliary activity: Propulsion of locomotory cells into the liquid environment and entrainment of a liquid on the surface of the tissue. Also, studies of ultrastructural morphology confirm the classical distinction between kinetocilli - active cilia, whose filamentary lining corresponds to the formula 9 + 2, and stereocyls (heterocycles) incapable of active movements possessing a filament set of type 9+ 0 [I.2] [I.5].

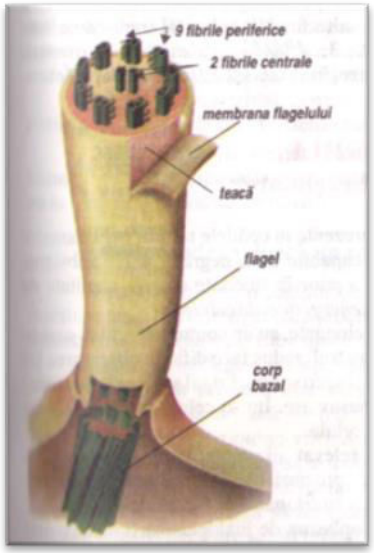

Fig.4 Flagellum structure[I.1]

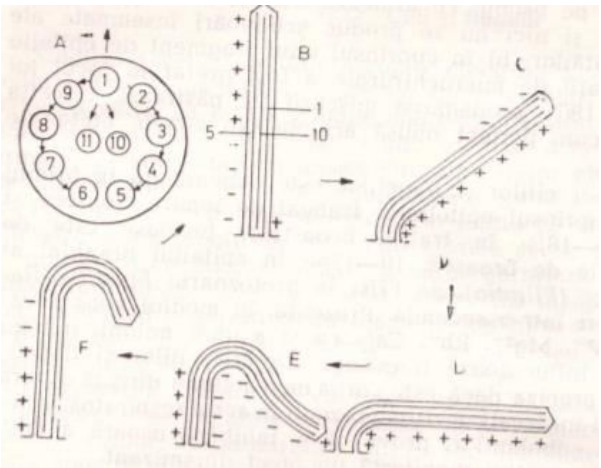

Fig.5 Mechanism of Cylinder Movement: A - arrangement of peripheral tubular (1-9) and central (10-11) pairs in a cross-sectional section - the arrows show the direction of impulse propagation in the filament system; B, C, D, E, F - successive positions of the target during a movement cycle; "+" - contraction; "-" – relaxation[I.1].

The movement of the flagellum starts at the base of the basal granule and propagates to the spike successively spreading to the peripheral fibrils (Fig.5A). Following the shortening of the fibrils 1, 2, 9, 3, 8 (FIG. 5B), the bow tilts before a rigid rod (Figure 5C) - is the active phase; In the phase of return, these fibrils relax, and the contraction occurs in the pairs of fibrils 4, 7, 5, 6, which provides an exactly opposite movement (Figs. 5D, E, F) and slower, contraction propagates more slowly in these last four pairs of contractile fibrils. After another hypothesis, during cilia bending, the tubular fibrils do not shorten by shrinkage, but only a sliding of one another relative to each other within the peripheral pairs. The biochemical basis of the movement of the cilia and the flagellums is quite incompletely established. Biochemical methods applied to flagellum by cytokine and X-ray diffraction studies revealed a protein-rich, lipid and carbohydrate-rich content; in the sperm tail, even the spermatine protein was separated, which would exhibit some properties similar to those of muscle contraction proteins. Like muscle fibrils, cilia and flagellums exhibit an intense ATPase activity, being able to hydrolyze the phosphate groups of ATP and, in particular, another nucleotide, adenosine-5-phosphate; they also exhibit succinic dehydrogenase and cytochrome oxidase activity, which are important in their energy metabolism; these enzymatic activities would be absent in the central fibrils. If ATP is added to the aqueous medium in which insulated flagellas are placed, they begin to perform waveforms.

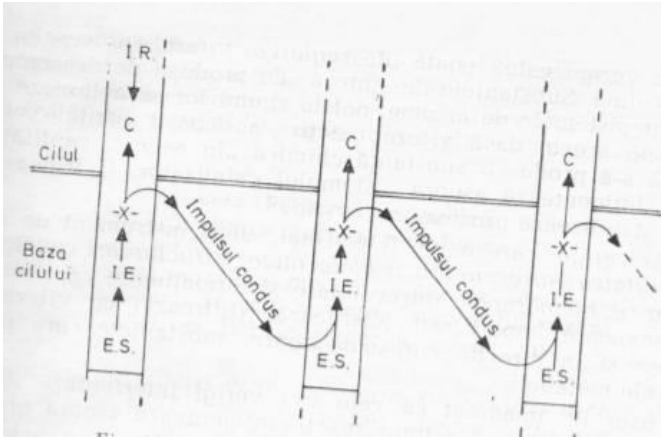

Fig.6 Mechanism of coordination of the I.R. - the initiating motif of movement; C- contraction; I.E. -Extension of excitation; S.E. - the occurrence of excitation; X- the impulse bifurcation zone[I.1]

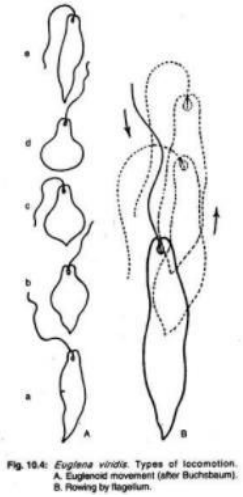
Fig. 10.4: *Euglena viridis*. Types of locomotion. A. Euglenoid movement (after Buchsbaum). B. Rowing by flagellum.

The metachronal and isochronal character of ciliary movements implies the existence of a coordination mechanism that would be accomplished in two stages: the occurrence of excitation within a motif and the conduction of excitation that targets more fibers. As shown in figure 6 there is an initiating motif of the movement and its rhythm: the impulse that is born propagates inside it at a determined speed, and then to the other fibers, successively [I.11].

Fig.7 Flagellum motion stages[III.8]

Starting from the biological

structure of the flagellum described above, it is possible to mechanically highlight the following structures similar to the flagellum, with the main purpose of favoring the aquatic movement.

a.*Elastic structure(Completly flexible)*

b. *Rigid structure*

c. *Hybrid strucutre*

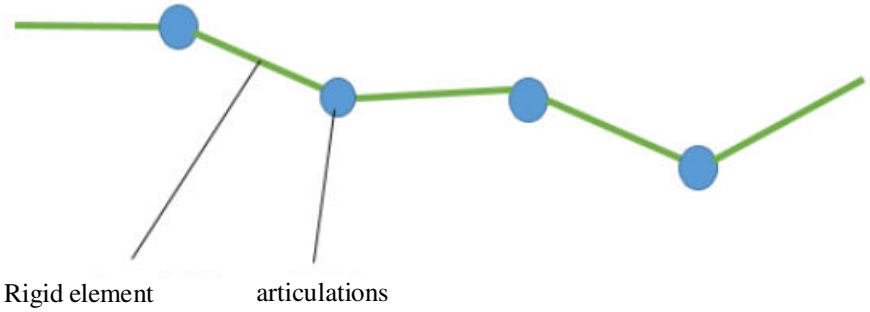

IV. Dinamic Scheme

Any electromagnetic wave is made up of an electrical and magnetic component, always oriented perpendicularly to each other, reporting wave polarization to the orientation of the electrical component. The stationary wave [III.1] is the physical phenomenon resulting from the overlapping of two waves of the same frequency in the same direction but in opposite directions, or in different directions. By interfering with the two waves, a constant wave structure is obtained over time. Waves that interfere to create a stationary wave can be of any kind: mechanical, sound, optical, electromagnetic, etc. The places where the resulting oscillation has minimal amplitude are called nodes, and the ones with maximum amplitude are called antinodes. Progressive waves distribute energy from a source point to a surrounding area, as vibrant particles or fields. Transverse vibrations - vibrations are perpendicular to wave movement - so if the wave moves horizontally, the vibrations will be in up and down. Longitudinal waves - vibrations are parallel to wave movement - so if the wave moves horizontally, the particles will

be compressed closer horizontally or horizontally expanded as they go (called the expanded bit a rarity). The movement of particles is a series of compressions and splinters, for example, similar to the sound and some earthquake waves.

Phase speed. From our usual experience of progressive water waves we know that they propagate at constant speed as long as environmental properties (water depth, for example) remain constant. When the waves are harmonic progressive waves, this velocity is called phase velocity v. We also know that the movement of a point in the z position at time t coincides with that of the point in z = 0 at a time before t', where t' is less than t with the time interval required for the wave to propagate over the distance z with the velocity v.

Thus, we can calculate the speed of these waves using the relation $v = f\lambda$. (1)

In the case of a continuous string, in which degrees of freedom are indices through the z parameter, the vibration amplitude of degrees of freedom in z can be written as a continuous function of z, denoted A (z). The form of A (z) as z function depends on mode;

That is, each mode has a different A (z). We can thus write the general expression of a stationary wave (2):

$$\psi (Z, t) = A (z) \cos (\omega t + \delta) (2)$$

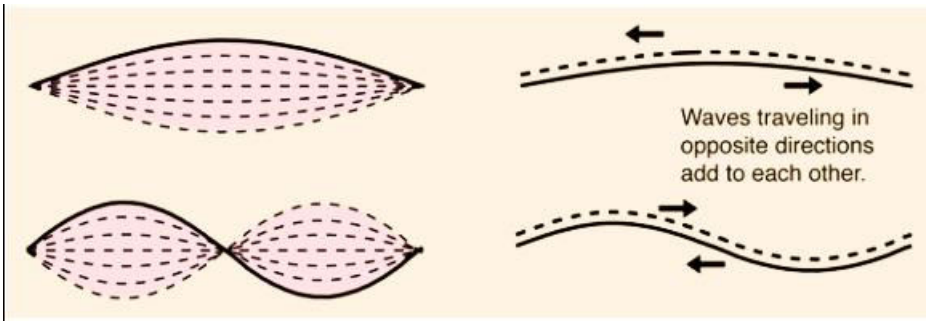

Fig.8 Examples of stationary waves[III.9]

Phase Relationship. The relative phase of two different moving points in an open environment in which a progressive harmonic wave propagates is very different from the one in the case of a stationary wave in a closed environment. In the case of a stationary wave, which may be a proper mode of free oscillation of a closed system or a forced oscillation of a closed system, all mobile points oscillate in phase with each other. This is not the case in a prognostic wave. If b moves farther from the external force than the mobile point a, then b executes the same movement as a but at a later time because of the time required to propagate the wave from a to b. Thus, b has a phase constant that differs from that of a by an amount equal to the product of the frequency and the time interval.

V. Identification of variants of electromechanical micro actuations similar to the flagellum movement

For critical analysis, the morphological method [I.7] will be used, determining the potential micro-actuations of the flagellum to be assessed [I.8], presented in the table below.

Tabel.1				
Types of actuations	**a.Elastic structure**	**b.Rigid structure**	**c.Hybrid structure**	**Score**
Micro DC motor	⁎⁎⁎	⁎⁎	⁎⁎	**7p**
Micro AC motor	⁎⁎⁎	⁎⁎	⁎⁎	**7p**
Electromagnets	⁎⁎	⁎⁎⁎	⁎	**6p**
Electrostatic actuation	⁎⁎	⁎⁎	⁎	**5p**
Piezoelectrical actuations	⁎⁎	⁎⁎⁎	⁎	**6p**
Magnetostrictive actuation	⁎⁎	⁎⁎⁎	⁎	**6p**
Termic actuation	⁎	⁎⁎	⁎	**4p**
Electrochemical actuation	⁎⁎	⁎⁎	⁎	**5p**
Hydraulic or pneumatic actuation	⁎	⁎⁎	⁎	**4p**

As can be seen from the scores in Table 1, the DC motor obtained the highest score, although options like piezoelectrical or electromagnetic actuations have a potential as well. Thus, the mainly actuation method used in laboratory experiments was the DC motor. The ratings were based not only on the interactions between the actuator and the structure but also on the power per space ratio and the power consumption of each type of actuator in different situations. The 1 star rating means that the actuator has either an inefficient power ratio or cannot interact at all with the proposed flagellum-like structures, while a 3 star rating not only has a potential good interaction but offers low power consumption when in load.

Following researches, the SRPS-1 engine (1), the JGB37-520 (2) and the vibration micromotor (3) were the most optimal selections, with the possibility to get a wider range of results from engine diversity. Before continuing with the use of these engines in future prototypes, we performed an analysis of the technical specifications for each of them.

1. SRPS-1 DC motor

This is a universal motor with the dimensions: 80x25x25 mm with a shaft with a length of 13mm and a diameter of 2 mm.

Fig.9 SRPS-1 engine

Voltage(V)	Current(A)	Torque(rmp)	Power(W)
2V	0,025	200	0,05W
4V	0,022	600	0,08W
6V	0,021	2200	0,12W
8V	0,022	4800	0,18W
10V	0,023	5500	0,23W
12V	0,022	6300	0,26W
14V	0,022	6700	0,30W
16V	0,022	7000	0,34W
18V	0,022	7800	0,38W
20V	0,021	8100	0,43W
22V	0,022	8600	0,49W
24V	0,024	9200	0,54W

Table.2 SRPS-1 engine specs

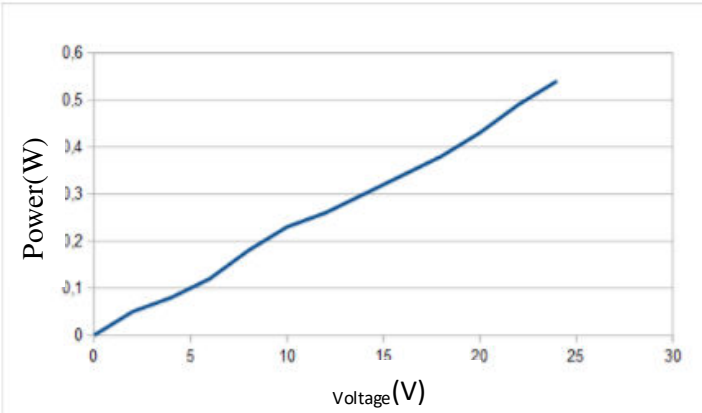

Fig.10 Current variation depending on the voltage applied to the motor

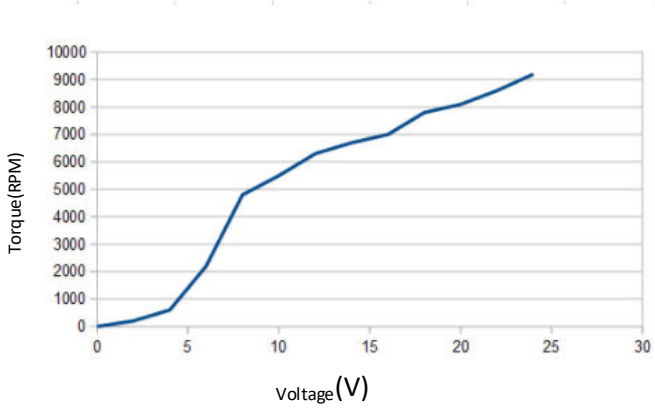

Fig.11 Power variation according to the voltage applied to the motor

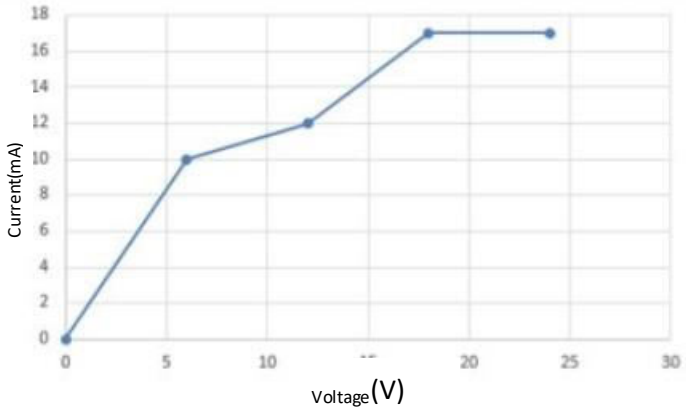

Fig.12 Variation of the speed in relation to the applied voltage at the motor terminals

For the SRPS-1 DC motor we have assessed 3 scenarios in which we evaluated the power(Fig.10), torque(Fig.11) and current(Fig.12) relative to the voltage applied on the motor's terminals. The graphs show that for achieving a high torque of over 8000RPMs the power consumption was relatively moderate but it required a high voltage drawn(around 20V) which represented an inconvenient since all the prototypes should be working with small batteries that an not deliver such voltages.

2. The JGB37-520 motor

JGB37-520 is a DC motor running at a supply voltage of 3-6 V (Volts). It has a weight of 150 g and the corresponding dimensions Fig.13.

Operating voltage: 3 V - 6 V
Rated voltage: 6 V
Current consumed when the engine is empty at 6 V: 300 mA
Current consumed when the engine is locked: 2 A
Current consumed when the motor is in charge: 700 mA
Nominal torque: 0.56 Kg * cm
Couple when the engine is locked: 2.20 Kg * cm

Fig.13 The JGB37-520 engine[III.10]

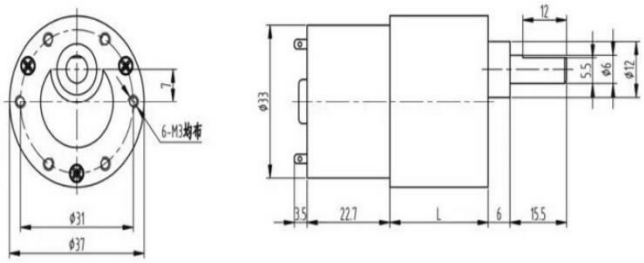

Fig.14 Engine dimensions JGB37-520[III.10]

3. Vibration Micromotor

The vibrating DC micro-motor is only 14mm in length and has an eccentric shaft in the form of a half cylinder, which is also the source of vibration generation.

The eccentric rotating mass or ERM vibration engine, also known as the pager, is a DC motor with an offset (unbalanced) mass attached to the shaft. As the ERM rotates, the centripetal force of the offset mass is asymmetric, resulting in a net centrifugal force, which results in a displacement of the engine. With a large number of revolutions per minute, the engine is constantly being displaced and moved by these asymmetric forces. This repeated movement is perceived as a vibration. Many mechanics manuals discuss the characteristics of ERMs as a "rotational imbalance" and do so in a negative context. The vibration produced by the ERM is an example of "powered harmonic vibration". This means that there is an external drive force that causes the vibration of the system, and this is sometimes called forced vibrations. The term "harmonic" means that the system is forced to vibrate at the frequency of excitation [III.5].

Fig.15 DC motor with vibration[III.5]

4. Vibration-encapsulated micro motor

This engine has a size of 7x25mm and has a principle of operation similar to the vibration engine described above, especially the overall capsulation that gives it waterproof and more hardness in case of shock exposure.

Operating voltage: 1.5-3V at a speed of 8000-24000 rpm.

With these specifications, the engine has an internal power of 0.01-0.06W with a torque of 0.3g.cm to 3g.cm (NM). These features make the vibration-encapsulated engine to be the best choice ever for aquatic displacement. Due to low current consumption, the motor can be used in small prototypes that do not facilitate high current sources.

Fig.16 DC motor with encapsulated vibrations[III.11]

5. Circular micromotor with vibration

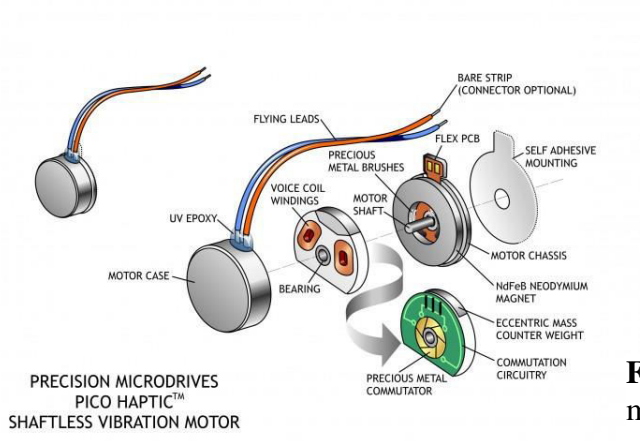

Coin vibration motors, known as vibratory motors without shaft or pancake, generally have diameters Ø8mm - Ø12mm. They integrate in several models because they do not have external moving parts and can be fitted with a permanent self-adhesive

Fig.17 Coin vibrant motor[III.12]

mounting system. Brush vibration motors are built from a flat PCB on which the 3-pole switching circuit is located around an inner center shaft. The vibration engine rotor is made up of two "voice coils" and a small table that is integrated into a flat, flat disk with a middle bearing on a shaft. Two brushes on the bottom of the plastic disc make contact with the PCB plate switch plates and provide the supply of voice coils that generate a magnetic field. This field interacts with the flow generated by a disk magnet that is attached to the engine chassis.

The switching circuit alternates the direction of the field through the voice coils, and this interacts with N-S pairs of poles that are embedded in the neodymium magnet. The disc rotates and, thanks to the built-in eccentric mass, the engine vibrates!

2. Electromagnets

The electromagnet as a temporary magnet whose action is determined by the passage of current through an excitation coil is based on the transformation of the electromagnetic energy into mechanical energy, giving electromagnetic forces at the level of the interferometer capable of acting on the movable armature. So the electromagnet can draw or reject the movable armature [III.4].

Characteristics of AC electromagnets - The Foucau hysteresis phenomena, through the currents that create them, produce a heating of the magnetic circuit, which is why the magnetic core is made of tolerances. In order to reduce shocks, the polar surfaces of the cores are rectified and a spiral is shorted to a magnetic field. They have a much higher operating gap than with DC electromagnets. The actual value of the current depends on the value of the interrupter. They have low self inductance relative to the supply voltage of the bobbin due to the high drive speed. It should be stressed that the shorting of a coil leads to the heating and the destruction of the coil while the continuous current only slightly changes the duration of the actuation and the return.

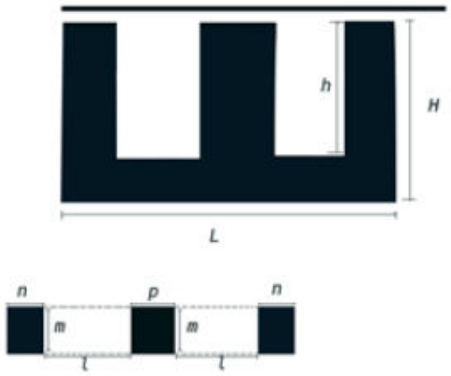

Fig.18 Reactive electromagnet model E

L(mm)	H(mm)	h(mm)	m(mm)	l(mm)	n(mm)	p(mm)
30.7	15.2	10.25	7.25	6.5	5.15	7.2

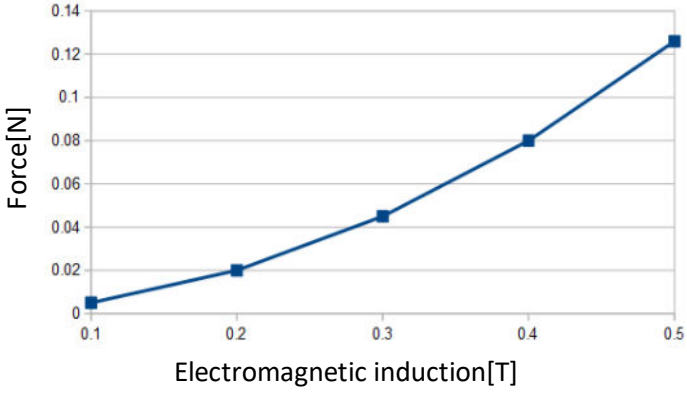

Fig.19 Graph of the dependence between magnetic induction and force

Induced force dependence table established following mathematical calculation based on the electromagnet used (Table.3).					
B [T]	0.1	0.2	0.3	0.4	0.5
F [N]	0.005	0.02	0.045	0.08	0.126

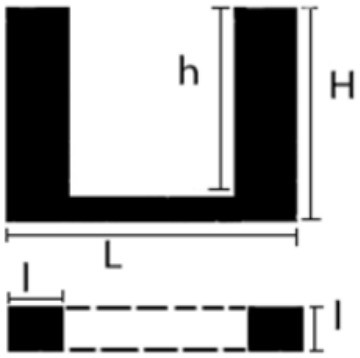

Fig.20 Electromagnetic resonator model U

L(mm)	l(mm)	H(mm)	h(mm)
20	**5.3**	**9.5**	**6**

$F = \frac{B^2 A}{2\mu_0}$ Where, B = Electromagnetic Induction

A = Section area

μ_0 = Constant disturbing

$B = \frac{U}{4.44 f A_f N}$ Where, U = Tension

N = number of turns in the coil

A_f = Area of the coil

f = Current frequency

With the above formulas we have calculated the force needed for the actuator of the extension and the induction of the circuit respectively. Resulting $F = \frac{1\times56,18\times10^6}{2\times4\pi\times10^7} = \frac{28,09\times10}{4\pi} == 2,236\text{N}$ and $B = \frac{5,3\times5,3\times2\times10^{-6}\times1.02}{4,44\times100\times56,18,\times200\times10^{-2}} = \frac{5\times10^2}{4,44\times56,18\times2} \cong$ 1T. After reworking one of the coils, replacing the 250 0.1mm diameter spirals with 500 spins of 0.05mm diameter, their parameters were measured with the results of Tables 4 and 5.

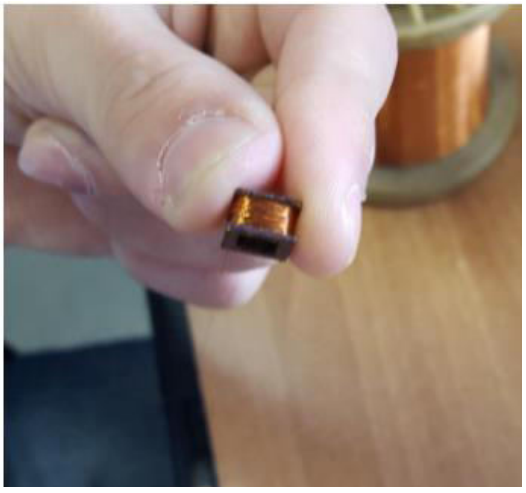

Fig.21 Coil made with copper wire of diameter 0.05mm

Tabel.4	Caracteristics 1	
	M.U.	Value
R[Ω]	f=120Hz	17.84
L[mH]	f=120Hz	7.44
R[Ω]	f=1KHz	81.7
L[mH]	f=1KHz	5.99

Tabel.5	Caracteristics 2	
	M.U.	Value
R[Ω]	f=120Hz	18
L[mH]	f=120Hz	7.5
R[Ω]	f=1KHz	83
L[mH]	f=1KHz	6.03

3. Piezoelectric actuation

A piezoelectric effect on a crystal compression take place at a temperature change ΔT that occurs in some piezoelectric crystals. The occurrence of an electrical polarization forming a potential difference with the generation of electric current. The piezoelectric effect is emphasized by the occurrence of an electrical potential difference at the ends of a dielectric or ferroelectric when a mechanical compressive force acts on it. The potential difference is due to the electrical polarization of the piezoelectric material under the deforming action of the external mechanical stress. Electric polarization consists in the appearance of electrical loads on the surface of the piezoelectric materials subjected to the action of the tensile forces.

The piezolelectric effect can be:

• directly;

• reverse;

Direct is when the monocrystalline materials are subjected to a mechanical pressure generating mechanical stresses and indirectly when under mechanical action a mechanical deformation occurs.

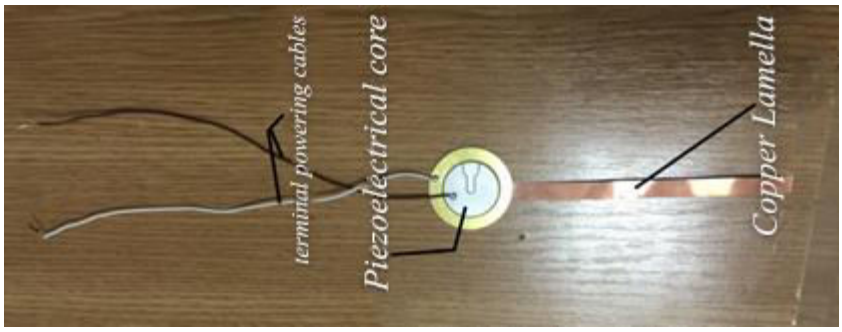

Fig.22 Piezoelectric actuator

The piezo-motor vibrations were recorded using an oscilloscope, after which several characteristics were analyzed and determined.

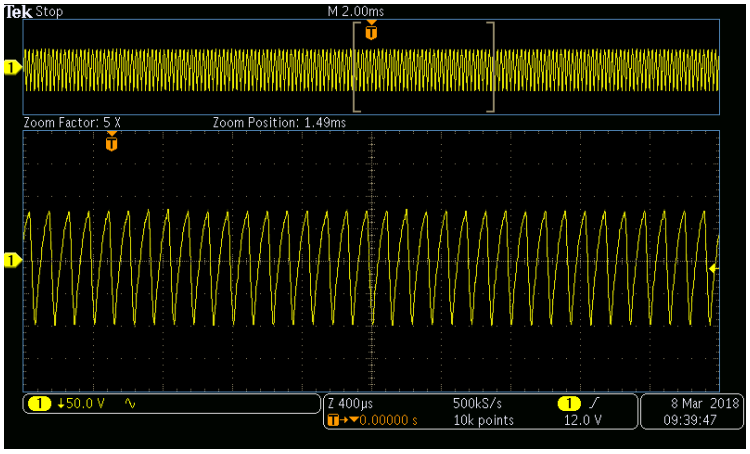

Fig.23 Oscillation produced by the piezo core

In order to achieve the piezoelectric drive, a copper assembly was used in the form of very thin blades. Thus, the vibration emitted by the piezo core was propagated according to Hook's law with F = kx, where k = the elastic constant
x = elongation / compression created

These actuation systems must interact with the three types of synthetic fibrillated structures;
a. Elastic structure
b. Rigid structure
c. Hybrid structure

VI. Experimental design

In order to achieve a representative model, some design laws must be respected. The prototype is composed of three planes: Body, half-breadth, and sheer. When floating in depth, the specific weight of the floating body is equal to that of the surrounding fluid, and when floating on the surface it is smaller. Hence, the property of a body to keep on the surface of the water, or under water, is called buoyancy. The result of hydrostatic forces caused by water pressure on the surface of the prototype is reduced to a vertical downward force Δm, called buoyancy force. It is equal to the volume of water deployed by the model [I.4]. At the same time, it is known that swimming at microscale requires techniques that are very different from those used by macroscale swimmers such as fish and humans [II.12].

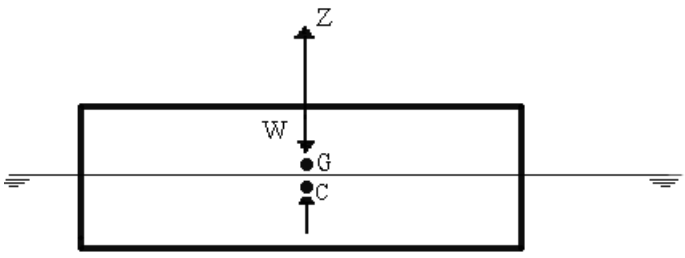

Fig.24 Action of hydrostatic forces and weight on the prototype

In prototyping, we considered the establishment of weight center, the decrease in the coefficient of finesse, and

the maximization of aerodynamics.

C – hull center

G – center of gravity

(5) G=$\rho \times V$ V=dispersed volume ρ= water density

$$G = \rho \times V = \frac{1g}{cm^3} \times 25cm^2$$
$$= 25g(the\ weight\ of\ the\ ship\ floating\ on\ the\ surface\ of\ the\ water)$$

The coefficient of flatness of the water line α is the ratio between its surface area and that of its circumscribed rectangle:

(6) $\alpha = \frac{A_w}{B*L} = \frac{2372}{94*31} = 0{,}81$, where A_w = floating area (mm^2)

B = width of circumscribed rectangle (mm)

L = length of rectangle circumscribed (mm)

The fineness coefficient of the master section, β, is the ratio between its immersed surface and that of its circumscribed rectangle:

(7) $\beta = \frac{A_M}{B*d} = \frac{27{,}2}{31*0{,}9} = 0{,}97$, where A_M = the immersed area of the master section (mm^2)

d = immersion (mm)

The coefficient of smoothness of the hull, ɤ, is the ratio between the volume of the hull V and the volume of the parallelepiped circumscribed:

(8) $\gamma = \frac{V}{L*B*d} = \frac{A_M*L}{L*B*d} = 0{,}97$, V = hull volume(mm^3)

The vertical fineness coefficient, χ, is the ratio between the hull volume and the cylinder volume, based on the water line area A_W and the draft as its height:

(9) $\chi = \frac{V}{A_w*d} = \frac{2556{,}8}{2134{,}8} = 1{,}19$

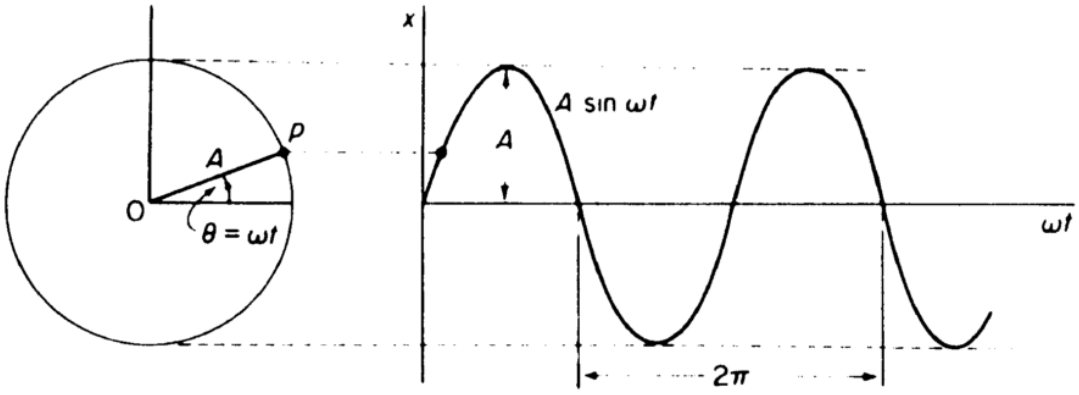

Fig.25 Transformation of circular motion into vibrations[III.5]

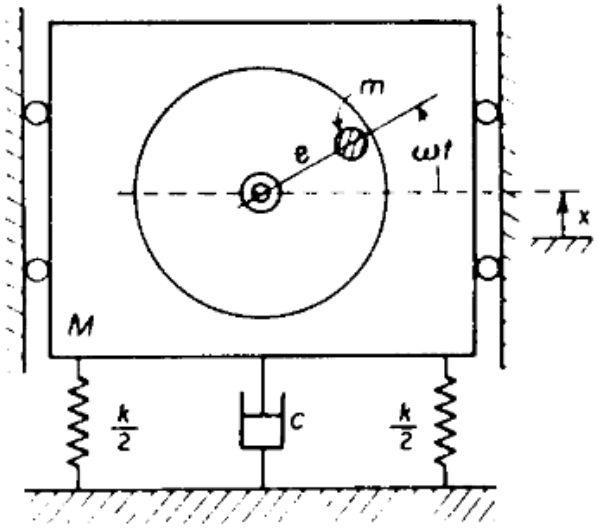

Fig.26 Engine diagram with vibration with a degree of freedom[III.5]

In the equations below, x is the displacement of the eccentric mass.

The above diagram (Fig. 26) has two separate springs, each with stiffness k2 representing a total stiffness k. This can be considered as a single k-arc that follows Hooke's laws, where F = kx. (10)

Viscous damping is proportional to mass speed

$$F = c\frac{dx}{dt}(11)$$

(speed is the derivative of the displacement).

The ERM mass (excluding the eccentric mass) follows Newton's second law of motion

$$F = (M - m)\frac{xd^2}{td^2}(12)$$

The sum of these three forces is equal to the entry F = F_0 sin (ωt) (13) .

Where F_0 is the centripetal force of the eccentric mass F = $mr\omega^2(14)$.

Here, m is the mass of the eccentric mass, and the equation is the distance from the motor axis to the center of the eccentric mass. This is sometimes called eccentricity and is referred to as an equation, such as in the diagram above. ω is the angular speed of the engine.

Now we have the motion equation for the system:

$$(M - m)\frac{d^2x}{d^2t} + c\frac{dx}{dt} + kx = F_0\sin(\omega t)(15).$$

We derived the equation of motion for an ERM vibration engine with a degree of freedom. On the components of this equation we can see that the force of the vibrations produced by the engine is affected by the mass of the eccentric weight, the distance between the eccentric mass and the motor shaft and the speed of rotation. The engine itself and what is embedded will also

affect the equivalent values for spring stiffness, damping characteristics and ERM mass, which in turn will influence the vibration level.

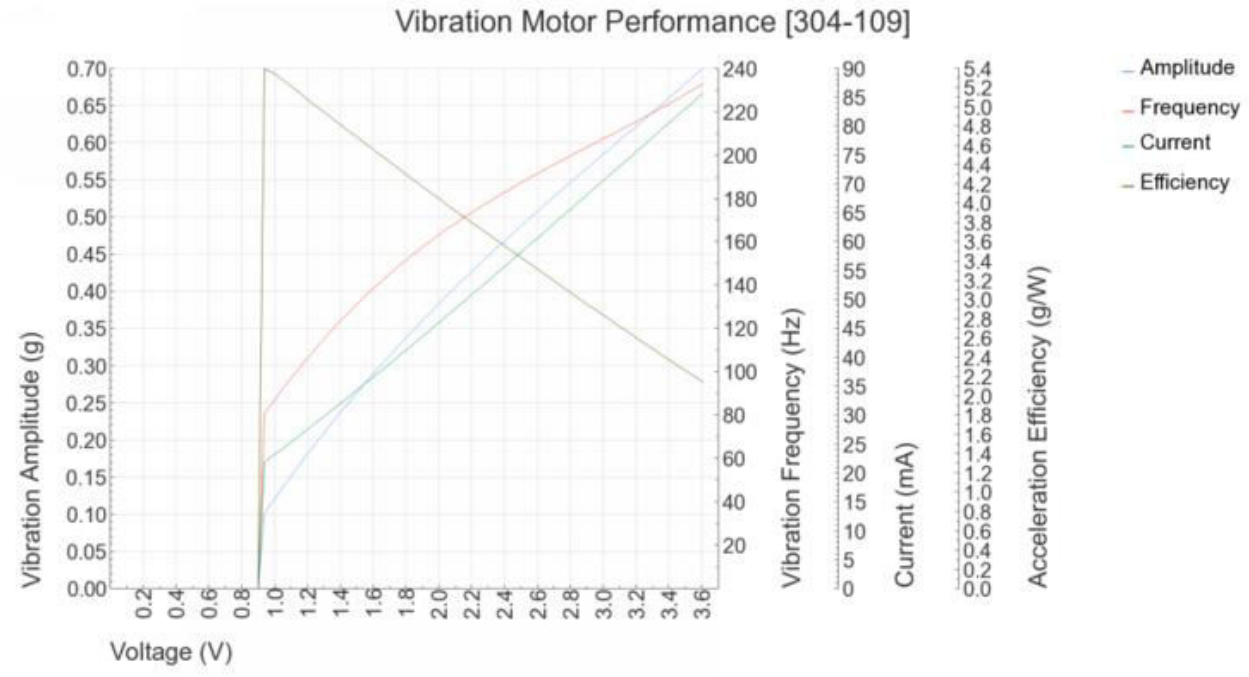

Fig.27 Graphic motor characteristics with vibrations[III.5]

For a long time it is known that swimming at microscoal requires techniques that are very different from those used by macroscale swimmers, such as fish and humans [II.12]. To understand this phenomenon, we return to the Navier-Stokes equations, which, in combination with the limit conditions, completely define a flow of fluid. For a constant density fluid ρ and a constant viscosity η, Navier-Stokes equations are given by a single vector equation, which can be undimensioned in space and time by the magnitude of the free flow V and a certain characteristic length L:

$$\left(\frac{\rho VL}{\eta}\right)\frac{dV}{dt} = -\nabla p + \nabla 2V \Rightarrow Re = \frac{\rho VL}{\eta} \quad (16)$$

V is the velocity vector field and p is the hydrodynamic pressure scalar field, both of which are not dimensioned[II.13]. From this equation we find Reynolds number, the non-significant amount that embodies the interaction between fluid inertia and viscosity. At Low, we are in a world that is either very viscous, very slow or very small. Low-Re flow around a body is called flow or Stokes flow. We do not see any more a turbulence transition, even behind the bluff bodies. At Re reduced, the role of time becomes negligible (II.12);

There is another factor to be considered in the microbubble: gravity. It is often said that inertia is negligible at low-Re, but "inertia" is used differently here than "mass". A microbot will reach its terminal speed in an almost instantaneous fluid, and the terminal speed decreases in size. However, even at low-Re, microrobot will still fall below their weight [II.12].

However, this only requires propulsion along the axis, which will be insufficient to counteract gravity during horizontal swimming, as shown in Figure 28 (a). It may be necessary to climb

with an attack angle, as shown in Figure 28 (b), similar to the way a helicopter flies. Microorganisms that swim with scabs have a similar density to water and are thus neutral, making this gravity effect on single helical propulsion for microrobots that are made of denser materials than water [III.6].

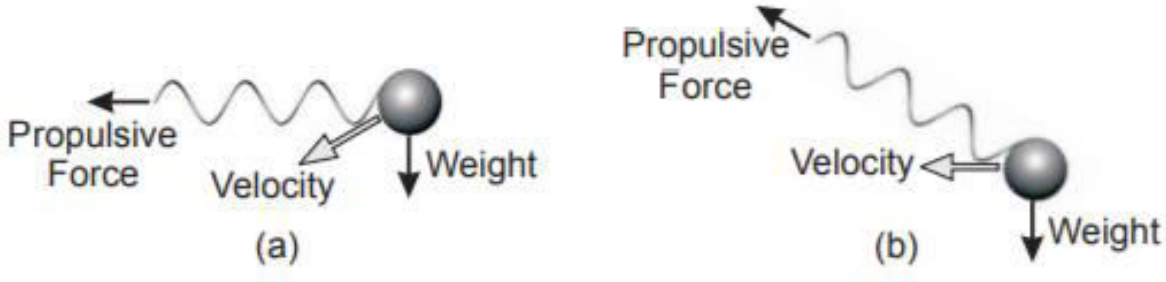

Fig.28 (a) Simple helical propulsion results in deviation due to gravity (b) Swimming like a helicopter flight can counteract gravity

VII. Development of experimental models of flagellar like micro robots

1st Experiment (DC motor).

Drive the synthetic fibril with the DC motor (SRPS-1).

Fig.29 Rotation movement of the fibril

Following a laboratory experiment involving the attachment of the fibrils to the SRPS-1 DC motor powered by the Rigolo DP1116 adjustable source, various methods of achieving a progressive wave were attempted. By attaching the flexible fibrils to the motor shaft and setting 3 axle clamping points, the following can be observed:

When the fiber was locked at one-third distance of the engine's axle, its movement was in the form of a small curved stand.

At half axis and three quarters, the distance from the moving fiber shaft remains constant in the form of a stationary wave (Fig.29), but its curvature increases. If the fiber is left freely in the air, due to the high speed of the engine it wraps around the motor shaft.

As a result of this experiment, it was found that little change is needed in terms of the fibril materials and properties. Thus, in order to obtain a progressive sinusoidal motion using the rotation motion of a DC motor, a stiff or a less curved fiber is required.

2nd Experiment (DC motor)

In this experiment I considered the JGB37-520 DC motor as a good source of interaction with the spiral aluminum fiber due to its low speed. Due to the large dimensions and the mass considerably high, we had to make a more voluminous tripod (cork) to have a higher water tension. So we decided to use a thin wooden cardboard with the dimensions of 260mm x 120mm. As it was not enough to support the engine's weight, we added a piece of 80x80mm expanded polyester, which offers a larger surface of water contact without hindering the ensemble. In order to balance the weight of the engine, which is located at one of the ends of the navy, we initially attached a weight of 10g, replacing it later with a 30g battery. The fibril was attached to the spindle motor, having an initial dimension of 285mm, shortened to 160mm later to reduce its contact with the lower boundary of the water tank. The engine was powered by an external 10000mAh battery with a 5V output voltage.

Thus, the calculated engine power was P = 4.6 V * 1 A = 4.6 W and the actual mechanical power: 80% * P = 3.68W.

Fig. 30 Prototype JGB37-520 engine in aquarium

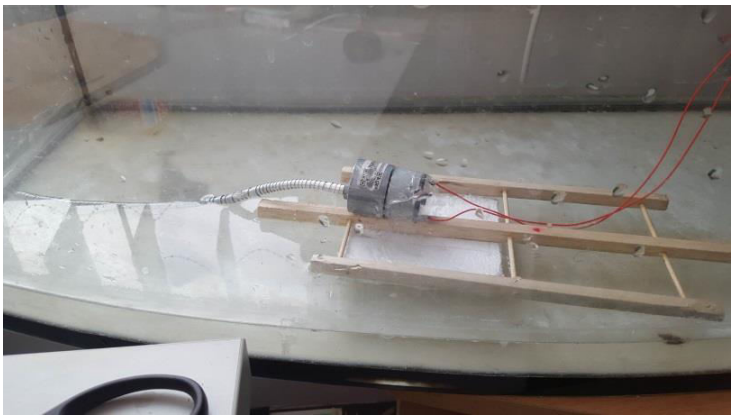

Fig.31 JGB37-520 engine prototype (2)

Following the experiments in the aquarium, it was found that due to the low engine speed, the aluminum spiral produces a thrust movement that generates circular waves. This motion produces a forward motion over a relatively small distance at speeds that do not exceed 1.1 cm / s. After which a spiral of the spiral appears, reaching the boundary of the basin.

To avoid this problem, we decided to ridge the aluminum filament by inserting two sticks of wood through it. So we still keep the thrust movement, eliminating just the coiling on the bottom of the basin.
After summarizing, I noticed that another important aspect in the movement of the protype is its mass. So with regard to the efficiency of the movement, we considered the prototype to be relieved by replacing the engine with SRPS-01 (Fig.32), with not only the smaller mass, but also the volume. To obtain the same speed, I powered the motor with a voltage of 2-3 V.

In conclusion of this experiment, we have found that the low speed of the DC motor stimulates the emergence of a forced type of progressive vibration. This prototype has achieved a progressive but uncontrolled movement, with difficulty handling in narrow aquatic environments due to the rotation of the monodirection. Thus, it has been noted a possible improvement of the positioning of two symmetrical motors at the anterior end, on the edges of the wooden structure and in the direction of rotation opposite one another, so that the two laterally acting forces are canceled, making the conditional displacement easy in different directions .

Fig.32 Experimental model with SRPS-01 motor and rigid aluminum spiral

3^{rd} Experiment (piezoelectric actuation).

In this experiment, we used a 20 V peak-to-peak voltage source, modifying the frequency value by 1000 Hz from 1 kHz to 20 kHz, delivering both visual and sound results in the 2000-3000Hz range. We then proceeded to a first exposure to the aquatic environment of the piezoelectric core using the hydrodynamic research tunnel (Chapter VIII).

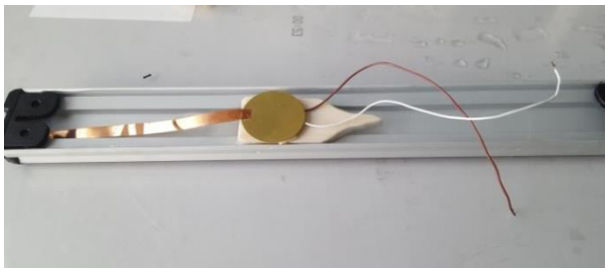

Fig.33 Piezoelectric prototype in the hydrodynamic tunnel

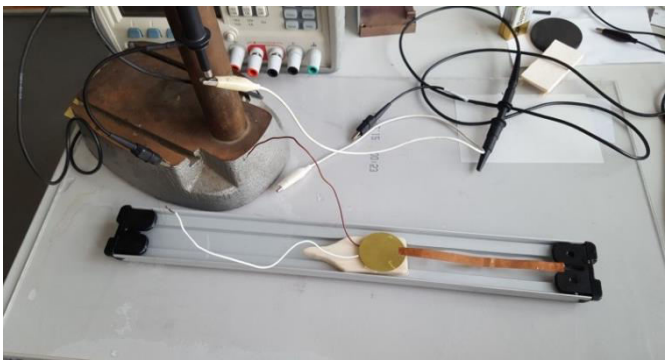

Fig.34 Piezoelectric prototype in the hydrodynamic tunnel(2)

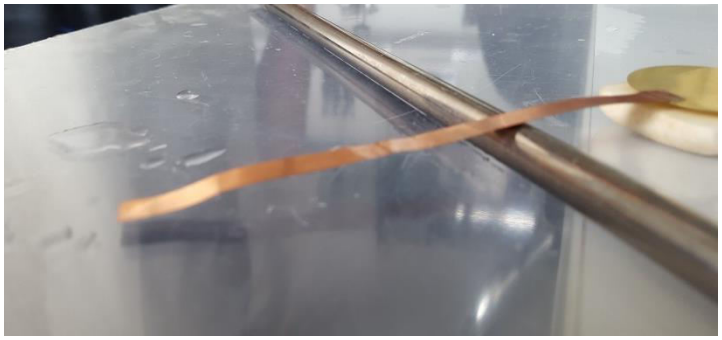

Fig.35 Method for highlighting vibrations at different frequencies using an aluminum rod to suspend the copper flap over the table

Following this experiment, it was found that the piezo core used did not generate a powerful enough impulse to propel and maintain the prototype in motion in the aquatic environment. To prove this, five different attempts were made to reposition the copper lamella to modify the intensity of vibration passing through the slat.

Observation (Fig.36): In this experiment the first interaction between the piezoelectric actuator and the aquatic environment was performed, resulting in secondary generation of semicircular waves along the copper strip when it is in contact with water by means of surface tension at the surface of the water but not when immersed in the liquid. The observation is considered to be noted and analyzed in a later experiment.

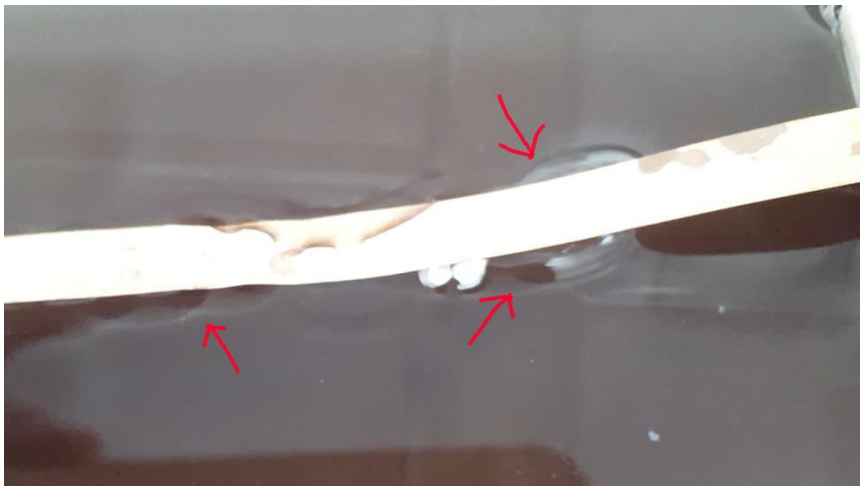

Fig.36 Wave on the surface of the water

4^{th} Experimentul (DC motor).

Making a micro robotic prototype that moves actively on the surface of the water with the help of the flagellum-like movement.
In the realization of this experiment was used a support made of cork, which presents, at the opposite end of the engine, an hidrodynamic design consisting of two curves with a sharpened head to provide easier penetration in the environment. For its operation, a 3V micromotor was used to which a 10 cm fiber was attached using a contractile barrel to maintain permanent

contact with the motor shaft (Fig.38). Following several attempts, due to the low torque of the engine, the prototype moved only in one direction, unevenly.

In table.7 below are presente the operational values ofr the DC micro motor prototype. The first movement with the synthetic (nylon) fibril can be ovserved vertically at a voltage of 2V. While the optimal state when it rotates horizontally it's only achievable at 3V with the motor being close to its maximim operating voltage limit. This shows that this motor may not be reliable at least not with a synthetic fibril since its weight considerably reduces the motor's torque, increasing the power consumption.

Tabel.7

U[V]	**I[A]**	**P[W]**	**Observations**
0.5	***0.016***	***0.01***	**Horizontally-does not rotate Vertically-does not rotate**
1	***0.032***	***0.03***	**Horizontally-does not rotate Vertically-does not rotate**
1.5	***0.048***	***0.07***	**Horizontally-does not rotate Vertically-does not rotate**
2	***0.061***	***0.12***	**Horizontally-does not rotate Vertically- it rotates**
2.5	***0.072***	***0.18***	**Horizontally-does not rotate Vertically-it rotates**
3	***0.083***	***0.25***	**Horizontally-it rotates Vertically-it rotates**

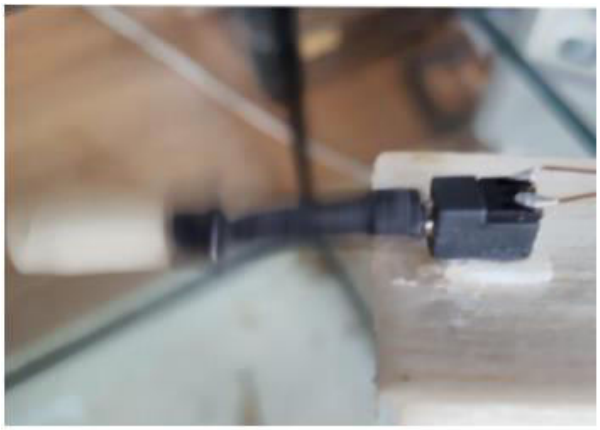

Fig.37 Micromotor spinning with the synthetic fibril

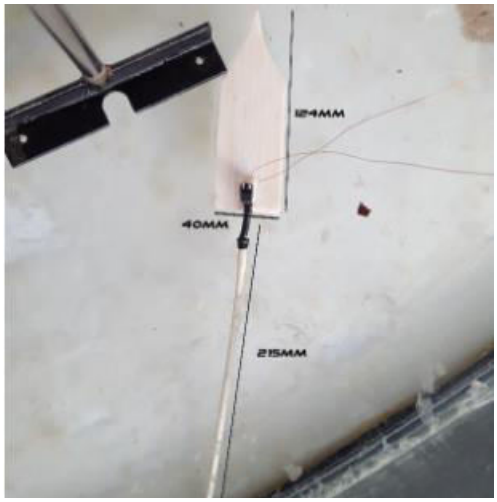

Fig.38 Experimental prototype

5^{th} Experiment (Vibration Engine).

For this experiment, we used an adaptation between experiments 2 and 3 using a vibration continuous current motor located on a copper slat with an extension, acting as a rigid flagellum-like structure. The principle of operation is that the micromotor has a high speed that produces vibrations due to the eccentric shaft so powered at 3V it transmits the vibration through the copper lamella which has an extension. This extension is in contact with water and vibrates vertically, generating a progressive wave that is sufficient to ensure the advancement of the prototype on the surface of the water and also features two floating sticks to give it a higher float.

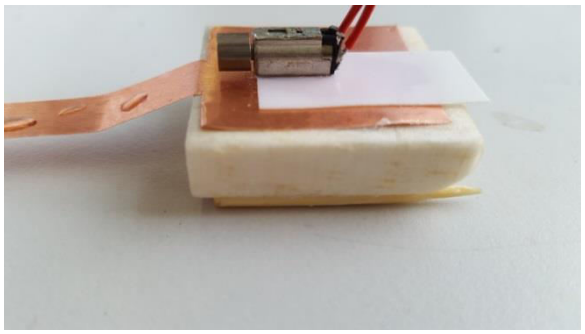

Fig.39 Vibration-driven prototype (lateral)

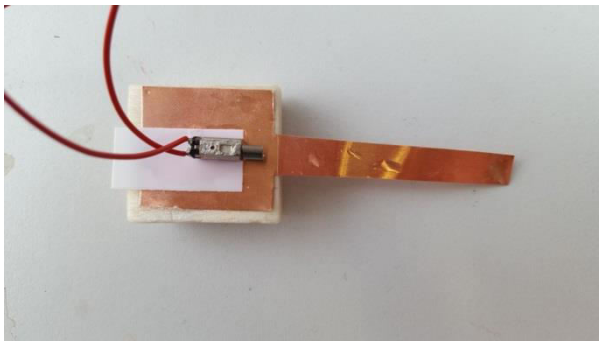

Fig.40 Prototype with displacement with vibration motor (top-down)

Following this experiment, promising results were obtained, being the first prototype to move on a straight line at a speed of 3cm / s (~ 11mph). In the continuation of this experiment we will also analyze the dependence between the different shapes of the copper lamella and the deformation velocity as well as the direction of movement, the subsequent prototype will have a larger surface and a higher buoyancy index in order to attach sensors data collection (such as ph, camera / vision, location, etc.).

For this model we have also developed a characteristic on the shape of the copper lamella, of which the most successful was the sinusoidal shape.

Fig.41 Sine wave - 1V supply voltage (forward travel)

Fig.42 Double sinusoidal form - supply voltage 0.8-1.2 V (uniform displacement with direction of rotation in the motor rotation direction)

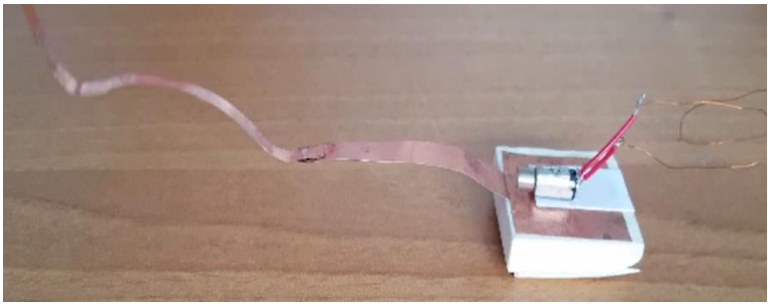

Fig.43 Suspended form - 0.8V supply voltage (stationary chaotic motion)

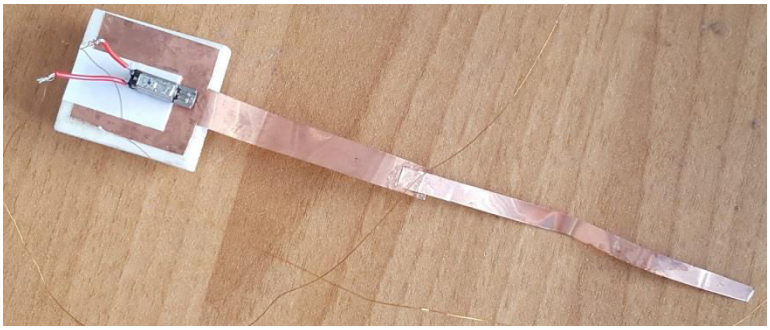

Fig.44 Straight form - 1.2V supply voltage

Speeds and displacements according to tail shape:

1. Sinusoidal:

Tabel.7

Time (seconds)	Voltage(V)	Distace (cm)	Speed(cm/s)
8	1	18	2.25
12.7	0.8	18	1.41
39	0.6	18	0.46
58	1.2	10	0.17

2. Straight

Table.8

Time (seconds)	Voltage(V)	Distace (cm)	Speed(cm/s)
18.5	1.2	18	0.97
20.6	1	18	0.87
>60	0.8	2-3	0.05

3. Suspended / floating

For 0.8V, 1V, 1.2V, prototype stagnation, no movement.

6^{th} Experiment (Vibration Capped Engine).

In this experiment we wanted to improve the aquatic movement through vibrations due to the promising results obtained in previous experiments. Using a vibration-encapsulated motor described in Chapter V - the DC drive section, which was inserted into a 3D print cartridge from the PLA and provisionally attached to a float for the purpose of compiling preliminary statistics. Table 9 shows the prototype characteristics in the aquatic environment.

Tabel.9

U [V]	0.5	1	1.5	2	3
I [A]	0.007	0.014	0.022	0.034	0.068
P [W]	-	0.01	0.03	0.08	0.2

We considered the 1.5V as the most optimal, achieving an acceleration of 0.006g under conditions of 24.8 ° C with a displacement of 0.13μm. Introduced in the water tank, the prototype recorded a horizontal-displacement with steering tendencies in the direction of rotation of the engine shaft, achieving an average speed of 2.4cm / s. Due to the high torque of the engine, the prototype has increased propulsion power, can even climb on dry surfaces (on the shore) and resist water turbulence.

This experiment has provided very good results for the state of the project, achieving a more advanced prototype shape with impermeability, greater longevity and improved power.

Fig.45 Vibration-driven prototype using encapsulated motor

7^{th} Experiment (Vibration Coin Engine).

In this experiment the same principle was applied, only that the copper lamella was attached vertically and with a narrower shape. A small coined-shaped vibration DC motor was used to power the device. The motor is powered by a 3V batter. The prototype manifested a small unbalance due to its low mass and the motor's high torque, but after securing the battery in place, the movement was straight. Due to its complete permeability, the prototype showed potential in movement not only on the water surface but even submerged.

Below in table 10 is a report of current and forces.

Tabel.10			
U [V]	1.5	2	3
I [A]	0.01	0.014	0.022
P [W]	0.01	0.02	0.06
F[cN]	-	0.25	0.4

This prototype reached speeds of 2.5cm/s at ½ size of the previous prototype. Also having a better actuation method that makes the control of direction (left , right) easier in the future.

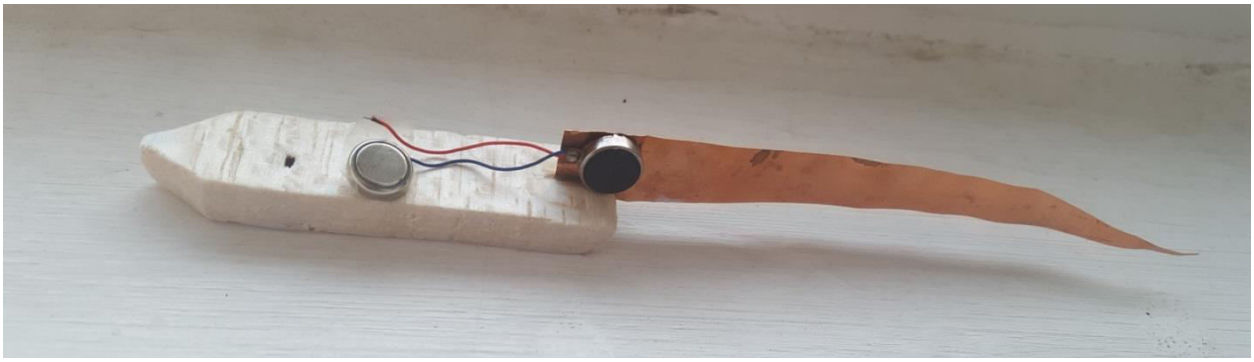

Fig.46 Coin vibration motor prototype

VIII. Designing and developing the necessary equipment for the characterization and testing of these types of unconventional micro actuations

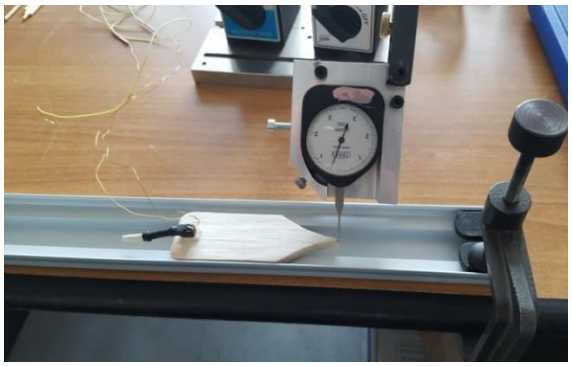

Fig.47.a Hydrodynamic Micro-Tunnel with Dynamometer

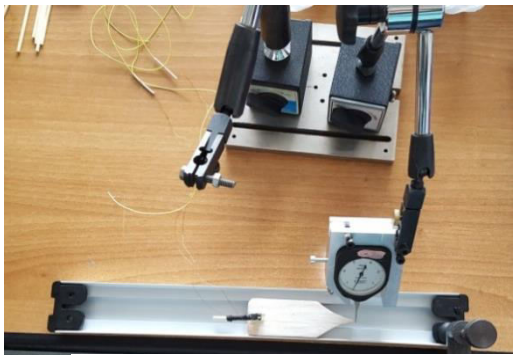

Fig.47.b Hydrodynamic Micro-Tunnel with Dynamometer

Fig.48 Micro-Tunnel hydrodynamic measurement of depth in water

To make a series of experiments to assess the prototype and establish some features, we have built a hydrodynamic tunnel that offers the possibility to add measuring elements (dynamometer, speed sensors, etc.). These experiments will determine the essential features of the prototype. The tunnel is made of stainless steel with a deep groove in the center. The ends are sealed by plastic supports that can be used to fix measuring elements or can be removed to connect other channels, thus increasing the size of the tunnel.

IX.a An experimental program to determine motion, speeds, accelerations under different climatic conditions for a complex characterization

For the purpose of an experimental study (research) it appeared the necessity of realizing some specific endowments in which the tunnel or the hydrodynamic stand was enrolled as the one presented above. An experimental protocol is proposed below.

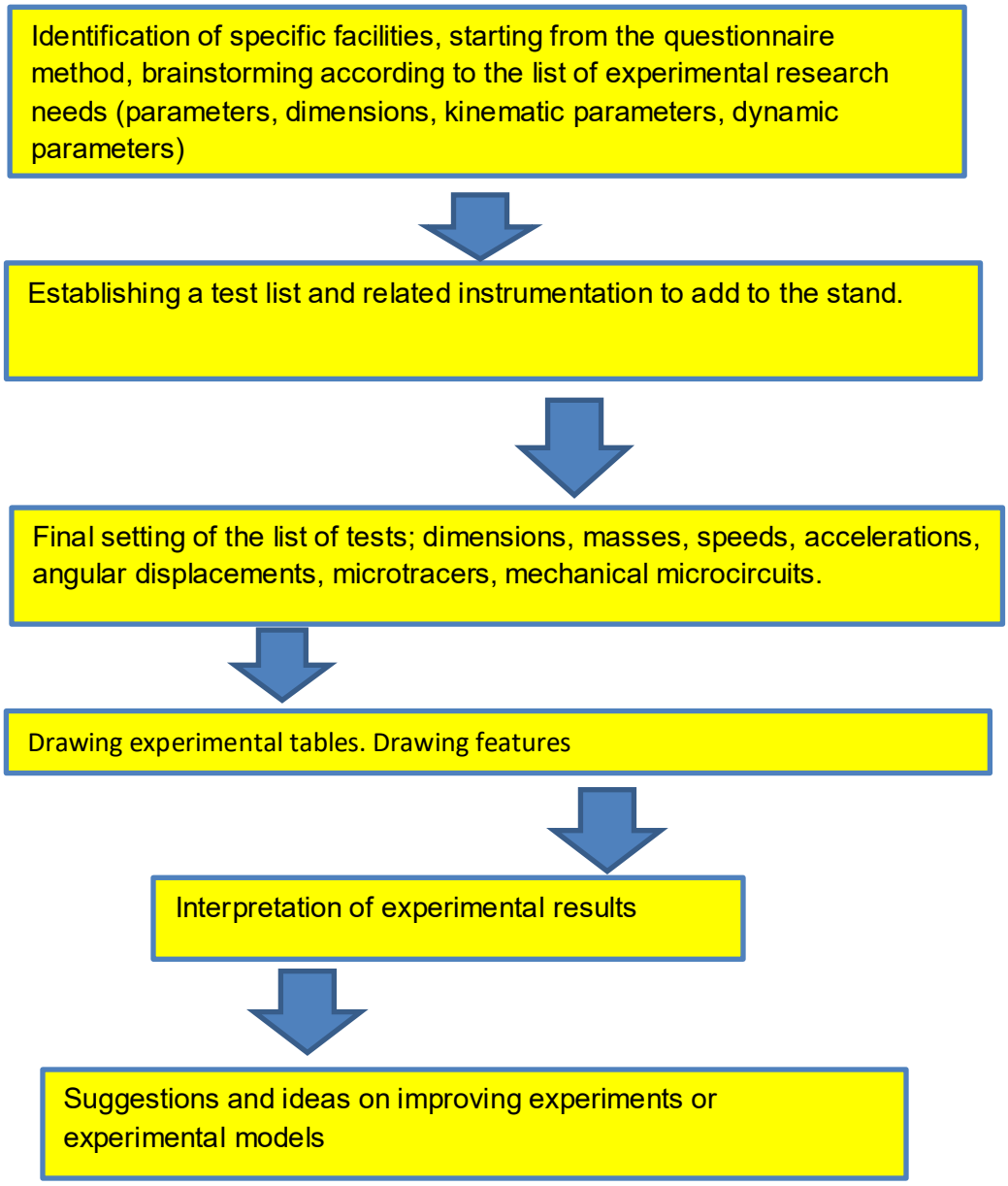

In order to properly follow the research algorithm, the appendix sections were established. At first I started with the questionnaire method that had the purpose to point out different aspects of the project prior to documentation stage. The Swot method followed, which served as an overall summary of the formerly progress. Before prototyping phase, I observed that a special testing controlled environment was needed, thus the brainstorming for an aquatic hydrodynamic micro-tunnel was initiated and ended up making a metallic frame tunnel based on the ideas generated.

IX.b Laboratory Equipment used

During the experimental phase multiple devices were used to measure and power different types of actuators.

- Rigol DP1116a DC Power Source (fig.49)
- Tektronix MDO3054 mixed Domain Oscilloscope 500MHz, 2.5 GS / s(fig.50)
- Fluke 287 true RMS Multimeter
- Micro Dynamometer max 4N, Pesola Elveti

Fig.49 DC Rigol DP1116a Rigol DC Power Source Used in the Laboratory for Experimenting Engines

Fig.50 Tektronix MDO3054 mixed Domain Oscilloscope used in measuring the piezoelectrical prototype

X. Identifying applications

Identifying applications.

- Aquatic monitoring methods (water level), regarding pollution, dynamic changes in the level of liquid, fauna or flora.
- Microchannel cleaning micro-technologies.
- Possible laboratory work on micro hydraulic dynamics, micro propulsion means.

XI. Conclusions

This project aimed at studying and understanding the movement of Green Euglena - an aquatic unicellular organism that, with the help of a flagellum, moves very efficiently in liquid media at microscopic level. We aimed to transpose the movement of this flagellum into mechanics by making prototypes with unconventional movement (especially vibrating direct current micro motors). At the design stage we designed prototype schemes and based on the calculation of the coefficients needed to accomplish the movement, we built the models presented in Chapter VI, following their improvement by adding a radio control system, environmental monitoring sensors, but also the capacity for submersibility.

APPENDIX 1

Questionnaire Method (1)

1. How does the travel mechanism work?
2. What kind of movement does it involve?
3.What are the environments in which to move?
4. Can it be introduced into the water?
5. Why does the eugene-robot move?
6.What speeds can touch and what are the factors that influence its speed?
7.What is the robot controlled?
8. How can it flow in different environments (water / dry)?
9.What kind of source is powered?
10.What is its autonomy?
11. What areas can be used?
12.What other practical goals can you have?
13. Being a bionic model, what class of flags did the main characteristics take over?
14.What factors would influence the project?

APPENDIX 2

Brainstorming method for aquatic hydrodynamic micro-tunnel

1. Measure the prototype speed (by timing the tunnel segment).
2. Making a spin rotation feature.
3. Force resistance.
4. Thrust force.
5. Increase fluid viscosity and experimentation under these conditions.
6. Characterization of the types of waves produced and their characteristics.
7. Determination of acceleration under difficult conditions.
8. Achieve a cinematic motion scheme.
9. Determination of the degree of immersion in the liquid.

APPENDIX 3

Swot Method

	STRENGHTS	WEAKNESSES
OPORTUNITIES	Due to many documentation sources it is possible to produce a representative bionic prototype for the flagelate class that can reproduce an exact movement and can be used in various fields such as medical,	The small dimensions of the materials for making the model and their quality in constrict with medium average liquids (water).
RISKS	Cessation of Center activity due to different reasons.	Carrying out the model using permeable materials that can damage this in liquid environments and also reduce use areas.

XII. Bibliography

I.Manuales

[I.1] V.Gh.Radu,V.V.Radu, "Zoologia Nevertebratelor" vlo.1, Litografia Învățământului, București, 1958.

[I.2] C.Wittenberger ,M.Keul ,"Mecanismele miscarii in lumea vie",Editura Academiei republicii socialiste Romane,Bucuresti 1987.

[I.3] Mircea Ignat,Gabriela Hristea,Gabriela Telipan,"Actuatori electromecanici si senzori neconventionali",Editura Electra,Bucuresti 2004.

[I.4] Viorel Handra-luca,Vistrian Mateis,Cornel Brisan,Teodor Tiuca,"Roboti structura cinematica si caracteristici",Dacia,Cjul-Napoca, 1996.

[I.5] E Dlazaroiu ,"Masini electrice de mica putere"Technica,Bucuresti 1965.

[I.6] Falie Vasile,"Manual de fizica clasa aIXa",Editura Didactica si Pedagogica,2011.

[I.7] Crum L.,”Ingineria inovării”.Ed.Tehnica,1986.

[1.8] Radulescu M.,Cimpeanu I.,”Masini si actionari electrice”,Ed.Scrisul Romanesc, Craiova, 1987.
[1.9] Voinea R.,Voiculescu V,”Mecanica mediului continuu.Aplicatii in ingineria”Ed.Academiei Bucuresti, 1989.
[I.10]Frank S. Crawford, "Unde" , Cursul de fizica Berkeley , vol.III , Editura Didactica si Pedagogica, Bucuresti 1983.
[I.11] Ilir H. Ionescu, Cimarron Ionescu, Mara Olimpia Ionescu, "Vademecum pentru modelisti" Editura Sport-Turism, Bucuresti,1983.
[I.12] Manual de Biologie clasa a-IXa, Ed Corint, Gh.Mohan,Gabriel Corneanu,Aurel Ardelean,2004.
[I.13] Biologie, Manual pentru clasa a IX-a, Nicolae Toma, Lucian Gavrila, Ed didactica si pedagogica-CNI CORESI, Bucuresti, 1999;

II. Impact publications

[II.1]G.Kosa, M.Shoham și M.Zaaroor "Propulsion Method for Swimming Microrobots" vol.23, nr.1, IEEE Transaction on Robotics, , februarie 2007.
[II.2]Iain A,Anderson,Thom Hale,Todd Gisby,Tokushu Inamura,Thomas McKay,Benjamin O'Breien,Scott Walbran,Emilio P.Calius,""Athin membrane artificial muscle rotary motor",Applied Physics A,iulie 2009.
[II.3]B T.Dickinson,"Hair receptor sensitivity to changes in laminar boundary layer shape",Bionspirations&Biomimetrics,vol 5,nr. 1,march 2010.
[II.4]Yingchen Yang,Nam Nguyen,Nannan Chen,Michael Lockwood,Craig rucker,Huan Hu,Horst Bleckmann,"Artificial lateral ine with biomimetric neuromasts to emulate fish sensing",Bionspirations&Biomimetrics,vol 5,nr. 1,march 2010.
[II.5]Yuanchang Liang,Minouri Taya,"Ferromagnetic Shape Memory Alloy Actuators",IEE Systems Journal,vol. 8,nr. 2,iunie2014.
[II.6]Ali Ghnabari,Ben Horan,Saeid Nahavandi,XiaoiQi Chen"Haptic Microrobotic Cell Injection System",IEE Systems Journal,vol. 8,nr. 2,iunie2014.
[II.7]T.E. Mengesha,R.R. Vallance and R.Mittal,"Stiffnen of desiccating insect wings",Bioinspiration&Biomimesis,vol.6,nr.1,March 2011.
[II.8]Frank Sanders,Barry A Trimmer an Jason Rife,"Modeling locomotion of a soft-bodied artropod using inverse dynamics",Bioinspiration&Biomimesis,vol.6,nr.1,March 2011.
[II.9]Q.Zhu,M.Moser and P.Kemp,"Numerical analysis of a unique model of locomotion:Verticalclimbing by Pacifc Lamprey",Bioinspiration&Biomimesis ,vol.6 ,nr.1, March 2011.
[II.10]John J.Socha,Kevin M.Klayz,Farid Jafari and P wlachos,"Non-equilibrium trajectory dynamics and kinematics of gliding in flying snake",Bioinspiration&Biomimesis,vol.5,nr.4,dec 2010.

[II.11]A.Teshigahara, M.Watanabe, N.Kawahara, Y.Ohtsuka, T.Hattori, "Performance of a 7-mm Microfabricated car" ,vol.4, nr.2, Journal of Microelectromechanical Systems, june 1995.
[II.12] E. M. Purcell. Life at low reynolds number. American J. Physics, 45(1):3–11, 1977
[II.13] J. J. Abbott, O. Ergeneman, M. P. Kummer, A. M. Hirt, and B. J. Nelson. Modeling magnetic torque and force for controlled manipulation of soft-magnetic bodies. IEEE Trans. Robotics, Accepted for Publication

III.Articles

[III.1] http://users.utcluj.ro/~mbirlea/x/07x.htm
[III.2]http://www.biologydiscussion.com/invertebrate-zoology/protozoa/euglena-viridis-habitat-structure-and-locomotion-protozoa/28141
[III.3]https://www.ncbi.nlm.nih.gov/books/NBK21698/
[III.4]http://aparate.elth.ucv.ro/Echipamente%20electrice%20I/Laborator/Studiul%20electromagnetilor.pdf
[III.5]https://www.precisionmicrodrives.com/content/ab-004-understanding-erm-vibration-motor-characteristics/
[III.6] https://www.telerobotics.utah.edu/uploads/Main/Abbott_ISRR07.pdf
[III.7] https://www.scribd.com/doc/151969114/Euglena-Verde
[III.8] http://www.biologydiscussion.com/animals-2/phylum-protozoa/study-notes-on-euglena-viridis-with-digram/32548
[III.9] http://hyperphysics.phy-astr.gsu.edu/hbasees/Waves/standw.html
[III.10]https://www.aliexpress.com/snapshot/0.html?spm=a2g0s.9042311.0.0.27424c4d77QscD&orderId=84441100859064&productId=32262772241
[III.11]https://www.aliexpress.com/item/7x25mm-Micro-Waterproof-Vibration-Motor-Coreless-Motor-Mini-DC-Vibrator-Motor-Professional MassagerMotor/ 32849172232.html?spm=a2g0s.9042311.0.0.27424c4dYpY3C1
[III.12] https://www.precisionmicrodrives.com/vibration-motors/coin-vibration-motors/